

# Annealed Polyelectrolyte Brushes under Normal and Lateral Compressions

C. Prinz, P. Muller, and M. Maaloum\*

*Institut Charles Sadron, Université Louis Pasteur, 6 rue Boussingault, 67083 Strasbourg Cedex, France*

*Received November 9, 1999; Revised Manuscript Received March 20, 2000*

**ABSTRACT:** We report here compression force measurements of diblock copolymers containing a short neutral hydrophobic sequence (polystyrene) and a long water-soluble weak polyelectrolyte sequence (poly(2-vinylpyridine)). This study focuses on the polyelectrolyte sequence and has been restricted to the case where the subphase is at pH 2. The lateral compressions were done using a Langmuir trough whereas the normal compressions were carried out with an atomic force microscope with a spherical particle attached to the tip. The thickness of the brush is considered as a function of the grafting density and is determined from the AFM force curves without reference to any theoretical model. At high grafting densities an "anomalous" behavior is observed, where the thickness of the brush decreases with increasing the grafting density. This is attributed to the annealed character of the polyelectrolyte.

## I. Introduction

The fundamental study of the interfacial properties of polymers in a confined state covers a large application domain, especially in the treatment of mud and the stability of sediments, domains where polymers play a prominent part. One area of interest is end-grafting (chemically) or end-adsorption (using the diblock copolymer), in which one end of a polymer chain is strongly attracted to the surface, while all other monomers are repelled. At moderately high surface coverage, the end-grafted polymers form a "brush", as the chains stretch away from the grafting surface. Brushes formed by uncharged polymers have been the subject of intense theoretical and experimental study in the past decade.<sup>1–10</sup> Attention has turned recently to charged polymer brushes. There exist two types of polyelectrolytes: the strong polyelectrolyte (or quenched polyelectrolyte) and the weak polyelectrolyte (or annealed polyelectrolyte). For quenched polyelectrolytes, the charges are fixed along the chain independent of the external conditions. On the opposite, the charge fraction of annealed polyelectrolytes can vary according to the external conditions such as the pH of the solution for instance. Most theoretical studies of polyelectrolyte brushes deal with quenched systems<sup>11–19</sup> and focus on the brush structure and the interactions between such brushes and either good or poor solvents. For sufficiently long and/or dense and/or charged brushes, the relevant terms in the energy have been found to be the osmotic pressure of the counterions and the elastic term. This regime has been qualified as "osmotic" by Pincus<sup>11</sup> and Zhulina et al.<sup>15</sup> These later gave the compression force profile of a brush in the "osmotic" regime. At strong compression, Pincus showed that the compression energy of polyelectrolyte brushes is dominated by the osmotic contribution of the counterions. So far only a few papers describing the properties of annealed polyelectrolytes brushes are available.<sup>20,22</sup> The effect of annealing for an individual polyion under poor solvent conditions was considered by Raphaël and Joanny.<sup>21</sup> For weak polyelectrolyte

brushes, the nontrivial effect of an increase in the brush thickness with decreasing grafting density  $1/\sigma$  is predicted by Zhulina et al.<sup>22</sup> They show that the thickness  $h_0$  of a brush scales as  $\sigma^{1/3}$ . This behavior is attributed to a local change of the pH inside the brush, causing a decrease in the polymer charge fraction.

Experimentally, it is difficult to obtain polyelectrolyte brushes. Only a few examples of a dense interface of polyelectrolyte can be found in the literature.<sup>23–27</sup> The long-range electrostatic interactions oppose in general the dense charged chains assembly, and in many cases, the copolymer adsorption can only take place in very salted water when the electrostatic forces are screened.

Herein, we study the annealed polyelectrolyte brushes at the water–air and solid–water interface using both Langmuir techniques and atomic force microscopy. We use the copolymer diblock polystyrene (PS)–poly(2-vinylpyridine) (PVP). Previous studies on PS–PVP/RX diblock copolymers where the PVP block, containing a paraffinic chain, is quaternized (quenched polyelectrolyte) showed that when the paraffinic chain contains several carbon atoms, surface micelles form at the air–water interface.<sup>28</sup> In our case, we show that the PS is anchored at the interface and the PVP is immersed in the water at pH 2. We present here for the first time the measurements of the forces needed to compress annealed polyelectrolyte brushes. The thickness of the brush has been determined as a function of the grafting density without reference to any theoretical model and compared to the theoretical results.

## II. Materials and Method

**Samples.** The brushes were made from a diblock copolymer composed of a short sequence of polystyrene (PS) and a long sequence of poly(2-vinylpyridine) (PVP) (Figure 1). The polystyrene is neutral, hydrophobic, and insoluble in water. The PVP is an annealed polyelectrolyte. The copolymers were provided by l'Ecole de Chimie des Polymères et Matériaux (ECPM, Strasbourg). They were synthesized by anionic polymerization. The average molecular masses of PS and PVP blocks are  $M_w = 18\,400$  g/mol and  $M_w = 166\,000$  g/mol, respectively. They have been determined by light scattering.<sup>29</sup> We also used an homopolymer of PVP containing 1352 monomers. This polymer was synthesized by radical polymerization at the ICS.

\* Author for correspondence: Tel (33) (0) 3 88 41 40 02; Fax (33) (0) 3 88 41 40 99; e-mail maaloum@ics.u-strasbg.fr.

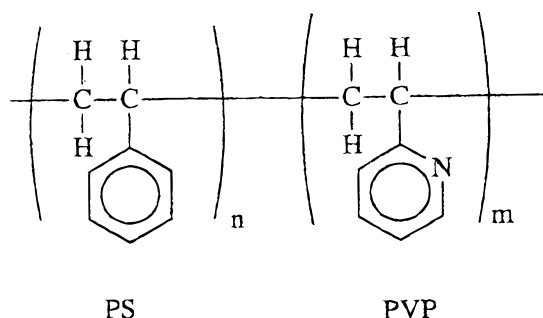


**Figure 1.** Chemical formula of the copolymers  $(PS)_n-(PVP)_m$ .

The PVP is only soluble in acidic aqueous solutions, where it acts as a weak base and acquires a net linear charge density due to protonation of the nitrogen in the pyrrolidine rings. It is well-known that for annealed polyelectrolytes, as a result of the buildup of an electrostatic potential, the  $pK_a$  is not constant but varies with both the degree of polymer protonation  $\alpha$  and the electrolyte concentration.<sup>30</sup> Elaissari et al. have estimated the degree of PVP protonation between pH 1 and 4.<sup>31</sup> The solubility of the PVP is limited to pH 4. At pH 2 the PVP is fully protonated ( $\alpha = 90\%$ ). Meanwhile, if we take into account the Manning condensation,<sup>32</sup> only the ions that are separated at a distance above the Bjerrum length are dissociated. This gives an effective degree of ionization  $\alpha_M$  for our polymer equal to  $\alpha_M = \alpha/l_B = 0.36$ , where  $a$  is the monomer size (2.5 Å) and  $l_B$  is the Bjerrum length (7 Å in water).

**Langmuir Isotherms.** The polyelectrolyte brushes are obtained by spreading the copolymer in a Langmuir trough (commercialised by Riegler & Kirstein), using water (Milli-Q from Millipore) at pH 2 (HCl from Prolabo is used) as the subphase. The spreading solvent is chloroform. The surface pressure is measured with a Wilhelmy plate.

**Langmuir-Schaefer Transfer.** Prior to any force measurement by AFM, the layer is transferred from the air-water interface to the solid-water interface using the Langmuir-Schaefer method.<sup>33</sup> The solid substrate used for this purpose is a silanized silicon wafer. The Schaefer method consists of positioning the silanized wafer parallel to the interface and then immersing it in the trough. The polystyrene strongly adsorbs on it, and the brush is then at the solid-liquid interface.

In the following, we assume that the brushes at the air-water interface are equivalent to those at the solid-water interface. This implies that only the grafting density and solution properties are determinant for the brush structure. This assumption is valid because at pH 2 the Debye length is of 3 nm, confirming that the image-charge effects are negligible in the brush. Then, the remaining problem to be solved is the determination of the grafting density of the brush at the solid-liquid interface. If the grafting density remains unchanged after the transfer onto the solid, then the equivalence between the "liquid" and the "solid" brush is valid. To estimate the transfer rate, a large solid surface is necessary. For geometry reasons, we used a silanized glass microscope slide of 19 cm<sup>2</sup> area. The slide is deposited at the water surface in the Langmuir trough (with the brush, at a given grafting density). We then expand the layer: the change in surface pressure in the expansion isotherm compared to the compression isotherm gives the number of remaining chains at the air-water interface. For the glass slide, we found that 90% of the chains corresponding to 19 cm<sup>2</sup> did not contribute to the isotherm anymore. Considering the accuracy of this method, we can conclude that the brushes at the solid-water and water-air interface have the same grafting density and thus the same properties.

**Atomic Force Microscopy.** All surface force measurements were obtained using a commercial atomic force microscope (AFM), Nanoscope III (Digital Instruments). For surface force measurements, it is necessary to determine the stiffness  $k$  of the cantilever. We have used the method described by

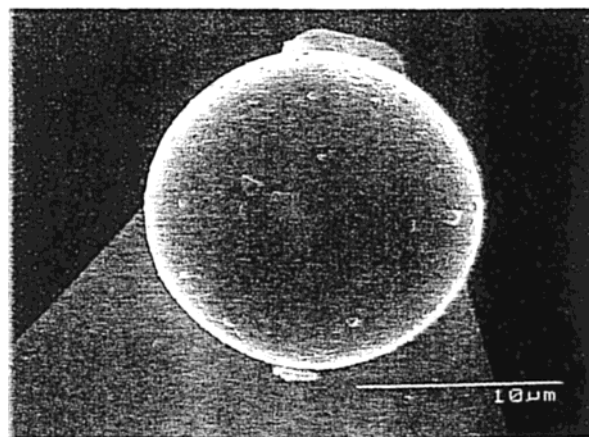


**Figure 2.** Scanning electron micrograph of a silanized glass sphere ( $R = 10 \mu\text{m}$ ) attached to the end of the cantilever.

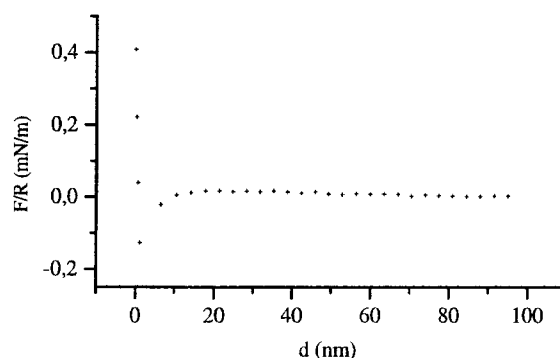


**Figure 3.** AFM force curve between a mica surface and a silanized glass bead. No repulsive electrostatic force is detected.

Senden et al.<sup>34</sup> Calibration of the spring constant, using this method, gave a value  $0.54 \pm 0.06 \text{ N m}^{-1}$ . In the experiments reported here, a silanized spherical glass particle of radius between 8 and 15  $\mu\text{m}$  has been attached to the end of the cantilever (Figure 2) so that the force is measured between the spherical particle and the polymer brushes grafted on the silanized silicon wafer. All force measurements were performed in water at pH 2, using a liquid cell.

The glass bead was silanized in order to eliminate the negative charges, and thus, we can exclude the long-range interactions from the experiment.

**Silanization of the Surfaces.** The silanization method is quite simple: the silicon wafers and the glass beads are washed in ethanol and dried with nitrogen before being left for 10 min in a silane solution. They are then washed again in ethanol and dried by water flux (because they are hydrophobic). The silane solution is composed of dimethylchlorosilane and cyclotetrasiloxane; it is commercialised by Pharmacia Biotech. The homogeneity of the wafer surface is then checked by atomic force microscope images in contact mode. This silanization method gives very homogeneous surfaces. To check whether the silanization method for the glass bead was successful, force measurement experiments were carried out with the silanized glass bead and mica surface. Figure 3 shows that after silanization no repulsive forces were detected.

### III. Theoretical Background

**1. Quenched Polyelectrolyte Brushes in a Salt-Free Solution.** Let us consider the situation of a planar surface in salt-free water, to which are grafted polyelectrolyte chains at a surface concentration of  $1/\sigma$ . Each chain contains  $N$  monomers of size  $a$ . A fixed fraction  $\alpha$  of these monomers is charged, and  $\alpha N$  counterions neutralize these charges. We can define the neutraliza-

tion length  $\xi$  as being the distance scale at which a test charge is screened in the layer. Let  $h$  be the thickness of the brush in a general way and  $h_0$  be the equilibrium height of the brush. Since excluded-volume interactions only play a significant role at very small values of  $\alpha$ ,<sup>12</sup> we can consider only the electrostatic and the elastic forces. Let us assume that all the chains are stretched homogeneously, that their ends are located at the outer boundary of the brush, and that the counterions distribution is homogeneous (simple box model). Two regimes may exist, according to Pincus:<sup>11</sup>

(a)  $\xi \ll h_0$ : **Osmotic Regime.** In this regime, the counterions are located inside the layer and  $\xi$  is the Debye length  $\kappa_{ci}^{-1}$  associated with the counterions' concentration:

$$\xi = \kappa_{ci}^{-1} = \sqrt{\frac{\sigma a}{4\pi l_B \sqrt{\alpha}}} \quad (1)$$

where  $l_B$  is the Bjerrum length (7 Å in water).

The osmotic pressure of the counterions, which is responsible for the swelling of the brush, is given by

$$\pi_{ci}(h_0) = kT\alpha c_p = kT \frac{\alpha N}{\sigma h_0} \quad (2)$$

where  $c_p$  is the monomers concentration,  $k$  is the Boltzmann constant, and  $T$  the temperature.

The elastic energy density is given by

$$E_{el} = kT \frac{h_0}{Na^2 \sigma} \quad (3)$$

At equilibrium, the force balance between these two contributions yields

$$h_0 = Na\sqrt{\alpha} \quad (4)$$

Bringuier showed that the surface pressure of such brushes is proportional to the osmotic pressure of the counterions  $\pi_{ci}(h_0)$ .<sup>35</sup>

Furthermore, in the osmotic regime, upon strong normal compression, the brush compression energy has been found to be equal simply to the osmotic pressure  $\pi_{ci}(h)$  of the counterions (see eq 2).<sup>11</sup>

Zhulina et al. developed a self-consistent-field theory (SCF) for the *osmotic* brush. They found that the compressed brush free energy is<sup>15</sup>

$$\frac{\Delta F}{kT}(h) = \alpha N \ln \left( \frac{3\pi\sqrt{\alpha}a^2}{\sigma \operatorname{erf}\left(\frac{h}{h_0}\right)} \right) \quad (5)$$

(b)  $\xi \gg h_0$ . In this regime, the counterions distribution extends beyond the layer. The neutralization length is equal to the Gouy–Chapman length  $\lambda$  corresponding to the charge density  $\alpha N/\sigma$ :

$$\xi = \lambda = \frac{\sigma}{2\pi l_B N \alpha} \quad (6)$$

The swelling of the layer by the counterions is now reduced by a factor  $h_0/\xi$ . The force balance between the swelling by the counterions and the elastic force now gives

$$h_0 = \frac{2\pi N^3 a^2 \alpha^2 l_B}{\sigma} \quad (7)$$

The *osmotic* brush regime is relevant for long chains and/or high grafting density, which is the case in our system.

**2. Quenched Polyelectrolyte Brushes in a Salted Solution.** Let us consider now the effect of added monovalent salt in the brush. Let  $C_S$  be the salt concentration. We can define the screening length  $\kappa_s^{-1}$  associated with the salt:  $\kappa_s^{-1} = 1/(8\pi l_B C_S)^{1/2}$ . In the case where the salt concentration is smaller than the counterions concentration, i.e.  $\kappa_s^{-1} > \kappa_{ci}^{-1}$ , the added salt has no effects on the brush.

On the other hand, if  $\kappa_s^{-1} < \kappa_{ci}^{-1}$ , the salt effects become important. Witten and Pincus<sup>36</sup> showed that, in the presence of salt, the osmotic pressure  $\pi_{osm}$  of a semidilute polyelectrolyte solution is given by

$$\pi_{osm} = kT C_{ci} \left( \frac{\kappa_{ci}}{\kappa_{ci} + \kappa_s} \right)^2 \quad (8)$$

where  $C_{ci}$  is the counterions concentration. In the *strong screening limit*, where  $\kappa_s \gg \kappa_{ci}$ , we obtain

$$\pi_{osm} = kT C_{ci} \left( \frac{\kappa_{ci}}{\kappa_s} \right)^2 = kT \frac{C_{ci}^2}{2C_S} = kT \left( \frac{\alpha N}{\sigma h_0} \right)^2 \frac{1}{2C_S} \quad (9)$$

The force balance between the osmotic pressure and the elastic force then gives

$$h_0 = Na^{2/3} \alpha^{2/3} \sigma^{-1/3} C_S^{-1/3} \quad (10)$$

The free energy of the compressed brush is given by

$$F = kT \left( \frac{\alpha N}{\sigma d} \right)^2 \frac{1}{2C_S}, \quad \text{for } h^* < d < h_0 \quad (11)$$

and

$$F = kT \left( \frac{\alpha N}{\sigma d} \right), \quad \text{for } 0 < d < h^* \quad (12)$$

where

$$h^* = \alpha N / 2\sigma C_S$$

The surface pressure of a salted brush is given by<sup>35,36</sup>

$$\pi = \frac{kT \alpha^{4/3} N}{4C_S^{2/3} a^{2/3} \sigma^{5/3}} \quad (13)$$

**3. Annealed Polyelectrolyte Brushes in the Osmotic Regime.** Zhulina et al.<sup>22</sup> have developed a mean field theory to describe the annealed brushes. They used the same model as above, except for the degree of dissociation of the polymer.

Let us assume that the polymer is a weak polybase. The dissociation of the base groups is governed by its dissociation constant  $K$  and by the concentration  $C_{H^+}$  of  $H^+$  ions in the brush. Let us suppose that the brush is immersed in an infinite reservoir of water with a fixed concentration  $C_{H^+}$  of  $H^+$  ions ( $\text{pH} = -\log C_{H^+}$ ) and a salt concentration  $C_S$ . We note  $c_p$  the polymer concentration in the brush,  $\alpha$  its dissociation fraction,  $\sigma$  the area per



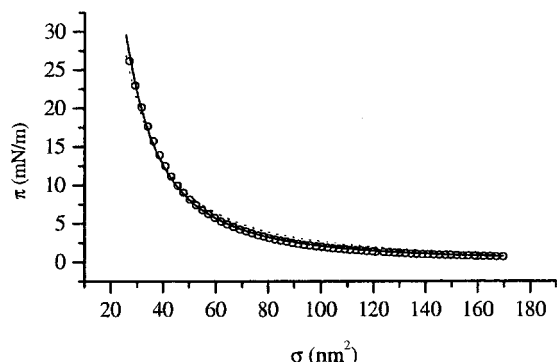


**Figure 4.** Langmuir isotherm of annealed (PS)<sub>177</sub>-(PVP)<sub>1581</sub> in water at pH 2. The  $x$ -axis is the area per chain in the brush. The circles represent the experimental points, the solid line represents the best fit of the surface pressure  $\pi \propto \sigma^{-2}$ , and the dash line represents the best fit of the surface pressure with the function  $\pi = A\sigma^{-5/3}$ .

chain, and  $\alpha_B$  the charge fraction of a single chain immersed in the bulk solution.

For  $\alpha c_p \gg (C_S + C_{H^+})$  and  $\alpha \ll 1$  (osmotic regime), Zhulina et al. found

$$\alpha = \sqrt{\frac{\alpha_B}{1 - \alpha_B} \frac{C_S + C_{H^+}}{c_p}} \quad (14)$$

and

$$h_0 = Na^{-4/3} \sigma^{1/3} \left( \frac{\alpha_B}{1 - \alpha_B} (C_{H^+} + C_S) \right)^{1/3} \quad (15)$$

The unusual law in  $\sigma^{1/3}$  for the thickness of the brush is related to the decrease of the charge fraction while reducing the area per chain. In fact, in the region of grafting chains, the polymer concentration increases when decreasing the area per chain  $\sigma$ ; as a result, the pH increases and the degree of ionization decreases. Consequently, the thickness of a brush decreases with increasing the grafting density.

The surface pressure of an annealed polyelectrolyte brush in the osmotic regime is given by

$$\pi = \pi_{\text{osm}} h_0 = kTNa^{-2/3} \sigma^{-1/3} \left( \frac{\alpha_B}{1 - \alpha_B} (C_{H^+} + C_S) \right)^{2/3} \quad (16)$$

#### IV. Results

Figure 4 shows the Langmuir isotherm of the PS-PVP spread on water at pH 2. The circles represent the experimental points, and the solid line represents the best fit with the function  $\pi = A\sigma^{-\beta}$ .

We have checked that the surface pressure curves are stable and represent the equilibrium state (at least on the time scale of our experiments). In fact, at different points on the curve we interrupted the compression, and the pressure remained constant. In the isotherm of the homopolymer PS, the surface pressure is decreasing very rapidly when the compression is interrupted as it has been shown by Kumaki.<sup>37</sup> Thus, in our case, the surface pressure is due to the PVP. We also checked that the layer was in a "brush" state at pH 2, i.e., that the PVP is not surface active at any grafting density. Figure 5 shows the PVP<sub>1352</sub> homopolymer isotherms at pH 2 (where the charge fraction is of 0.9) and at pH 6 (where the polymer is neutral). The homopolymer does not

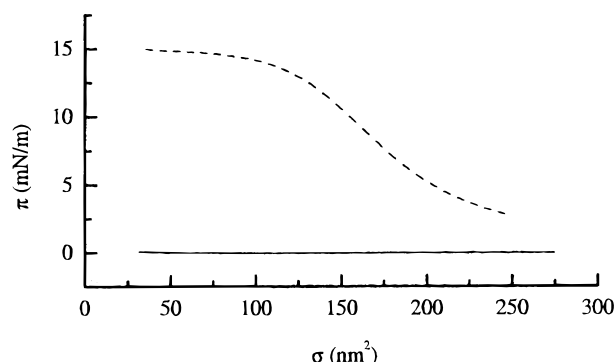


**Figure 5.** Langmuir isotherms of annealed PVP<sub>1352</sub> in water at pH 2 (solid line) and pH 6 (dash line). The  $x$ -axis is the area per PVP chain.

generate any surface pressure at any grafting density at pH 2 while its surface pressure is increasing at pH 6 until it reaches a plateau. Thus, we can conclude that at pH 6 the PVP chains are adsorbed at the interface at big areas per chains and that there is a compression-induced solubilization of the polymer at the plateau while at pH 2, the PVP chains are completely solubilized. We can therefore exclude the formation of surface micelles at pH 2.<sup>28</sup> This implies that, at pH 2, after spreading the copolymer in a Langmuir trough the PVP sequence goes into water, and the PS sequence plays the role of the anchoring point, preventing the PVP sequence from going into the bulk. The pressure observed in Figure 4 is due only to the interaction between charged PVP chains forming a brush at the air-water interface. However, we cannot exclude completely the formation of micelles at the interface, but their effects would be negligible since the length of polyelectrolyte sequence is 10 times higher than that of polystyrene. Note that Zhu et al.<sup>28</sup> have observed that when the paraffinic chain attached to the PVP contains only one carbon atom, which is similar to our system, the polyelectrolyte PVP/C<sup>+</sup> chains, being very water-soluble, assume a subphase conformation perpendicular to the interface.<sup>28</sup>

Surprisingly, the best fit of the isotherm shows that the surface pressure of the brush scales as  $\sigma^{-2}$ . For an annealed polyelectrolyte brush, we would have expected a scaling law in  $\sigma^{-1/3}$ , as predicted by Zhulina's theory (cf. eq 16). On the other hand, the exponent ( $-2$ ) is close to  $-5/3$ , which is predicted for a quenched polyelectrolyte brush in the strong screening regime. At pH 2, the concentration of the H<sup>+</sup> ions arising from the chlorhydric acid added in the solution is equal to  $10^{-2}$  M. Then we can consider that the salt concentration is high enough so that the brush is not in the osmotic regime dominated by the counterions, but in the "salted" regime, where the degree of dissociation is fixed. The dashed line in Figure 4 represents the best fit using the function  $\pi = A\sigma^{-5/3}$ , which gives  $A = 7.8 \times 10^{-30}$  N m<sup>7/3</sup>. Since we have  $A = (kT\alpha^{4/3}N)/(4C_{H^+}^{2/3}a^{2/3})$  (cf. eq 13), we can deduce the value of the charge fraction  $\alpha$  from the prefactor  $A$ . Taking  $C_{H^+} = 6.04 \times 10^{24}$  m<sup>-3</sup>,  $a = 2.5 \times 10^{-10}$  m,  $kT = 4 \times 10^{-21}$  N m, and  $N = 1581$  gives  $\alpha = 0.12$ . This value is below the threshold given by Manning condensation ( $\alpha_M = 0.36$ ). Similar phenomena have been observed for quenched polyelectrolytes in dilute solution.<sup>38</sup>

To study the force required to vertically compress the brush with the silanized glass particle in aqueous

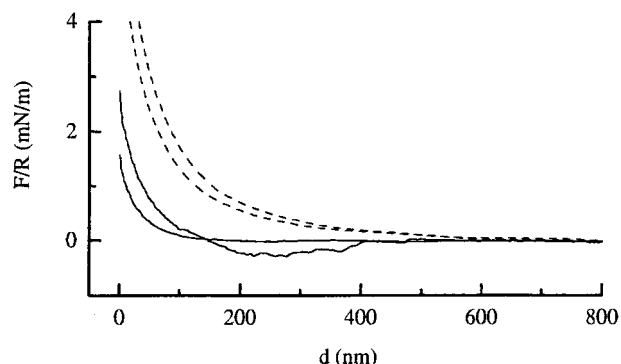


**Figure 6.** AFM force–distance curves for the (PS)<sub>177</sub>–(PVP)<sub>1581</sub> brush in water at pH 2 at a grafting density of  $2 \times 10^{-3} \text{ nm}^{-2}$ . The curve in solid line corresponds to the first scan, and the dashed line was obtained after a big number of scans (approximately 100).

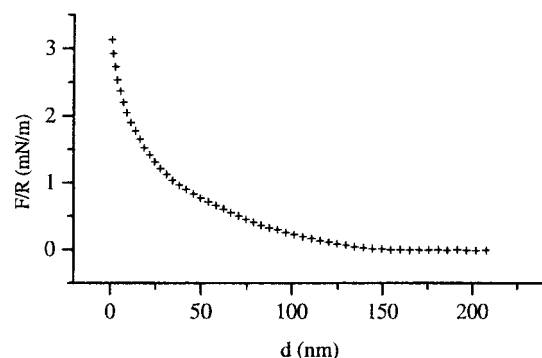


**Figure 7.** AFM force–distance curve for the (PS)<sub>177</sub>–(PVP)<sub>1581</sub> brush in water at pH 2 at a grafting density of  $2.86 \times 10^{-4} \text{ Å}^{-2}$ .

solution at pH 2, we transferred the brushes to the silanized silicon wafer surface using the Schaefer method.

Figure 6 shows two AFM force–distance curves obtained on a brush at a grafting density of  $2 \times 10^{-3} \text{ nm}^{-2}$ . The curve in the solid line corresponds to the first scan, and the dashed line was obtained after a big number of scans (approximately 100). For both curves, the compression force is always repulsive. For the dashed curve, the force is detected at a distance of 600 nm, which is bigger than the contour length of a single molecule ( $Na = 396 \text{ nm}$ ). Since we have silanized the glass bead in order to exclude long-range electrostatic interactions from our measurements, we can conclude that there is a polymer transfer from the wafer to the sphere. This is confirmed by the observed jumps in the force measured during the separation of the two surfaces. Thus, in what follows, we considered only the force–distance curves corresponding to the first scans. The AFM tip was changed, and another region of the brush was explored each time we observed some bridging during the separation. The force curves obtained for different regions of the sample and on various brushes at the same grafting density are identical.

Figure 7 represents a typical AFM force measurement between the particle and the brush. In this case the brush was transferred onto a solid surface with a grafting density  $1/\sigma = 2.86 \times 10^{-2} \text{ nm}^{-2}$ . We repeated the same experiment on brushes at various grafting densities. We then tried to fit the different force profiles obtained using the theories given in section III. Although each curve could be well fitted by the theoretical functions, the parameters did not vary in a satisfying

way with the grafting density. This implies that additional effects than those taken into account in the presented theoretical models could play a role in the polyelectrolyte brushes. For instance, it has been shown that for annealed polyelectrolytes the charges are not distributed homogeneously along the chain.<sup>39</sup> This effect could dramatically affect the force profile. Therefore, we have determined the thickness of the brush in a way that is independent of any theoretical model. The thickness of the brush  $h_0$  is taken as

$$h_0 = d_0 + h_1$$

where  $d_0$  is the distance at which the repulsive force is detected on the AFM force curves, and  $h_1$  is the thickness of the brush at the maximum compression.

We assume that  $h_1$  is the dry thickness of PVP at the given area per chain  $\sigma$ , that is,

$$h_1 = \frac{m}{\sigma \rho}$$

where  $m = 2.75 \times 10^{-19} \text{ g}$  is the mass of a PVP chain, and  $\rho = 0.95 \text{ g/cm}^3$  is the PVP density. This method of determining the thickness of the brush is justified since (i) we compress the brush with a hydrophobic spherical particle, so we have no electrostatic interaction between the brush and the particle, and (ii) the chains are very long compared to the Debye length and all the counterions are concentrated inside the brush. We then determined the thickness of the brush at a given grafting density by calculating the average value of the thickness obtained on 30 force curves. For a given brush, the maximum difference between the values of the thickness obtained on different curves is equal to 10 nm. As a consequence, we consider that the uncertainty in  $h_0$  is of the order of 10 nm.

Figure 8b shows the brush thickness determined with the method described above as a function of the grafting density. Three different regions are distinguishable (I), (II), and (III). The brush thickness  $h_0$  is stable in region (I), at a value  $h_0 = 130 \text{ nm}$ . In region (II),  $h_0$  increases with decreasing  $\sigma$  and exhibits a maximum at  $\sigma = 120 \text{ nm}^2$  per chain before decreasing rapidly with decreasing  $\sigma$  in region (III). In region (I), the distance between the chains is large so that they behave as if they were alone at the interface. This explains the constant value of  $h_0$  in this region. The increase of  $h_0$  with decreasing  $\sigma$  in region (II) may be explained by the electrostatic repulsion between the chain or by an increase of the osmotic pressure of the counterions, due to the reduction of the area per chain. In the region (III), the dependence of  $h_0$  on  $\sigma$  has never been observed experimentally before. It is an “anomalous” behavior for polymer brushes. This behavior has been predicted by Zhulina for annealed polyelectrolyte brushes in the osmotic regime.<sup>22</sup> The solid line in Figure 8b represents the best fit of  $h_0$  with the function  $h_0 = B\sigma^x$ . The best fit gave  $x = 0.31 \pm 0.02$ , which is in agreement with the theory (cf. eq 15). According to the prediction of Zhulina, the decrease of the brush thickness with increasing grafting density in region (III) can be related to the decreasing degree of ionization. In fact, inside the brush, the polymer concentration increases with the decrease in  $\sigma$ ; as a result, the pH increases and the degree of ionization decreases. Consequently, the thickness of the brush decreases with decreasing the area per chain  $\sigma$ .

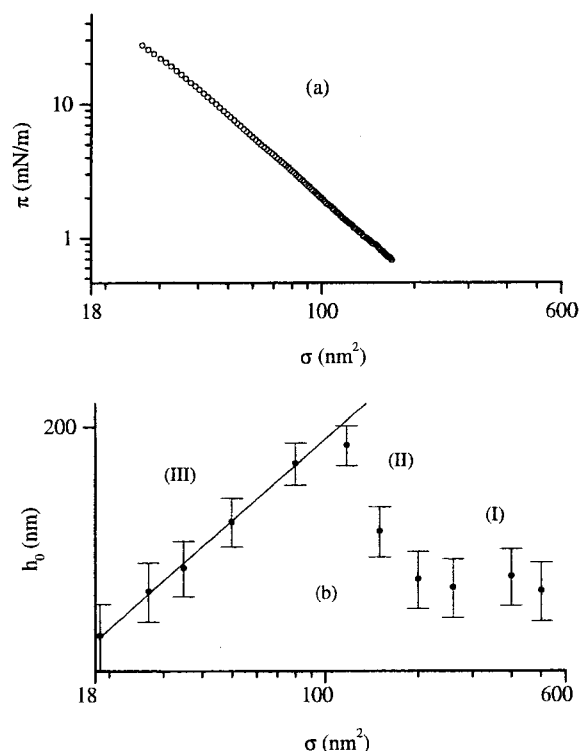


**Figure 8.** (a) Langmuir isotherm of annealed (PS)<sub>177</sub>-(PVP)<sub>1581</sub> in water at pH 2 in a double-logarithmic representation. (b) Equilibrium thickness of the (PS)<sub>177</sub>-(PVP)<sub>1581</sub> brush in water at pH 2 as a function of the area per chain in a double-logarithmic representation. The solid line represents the best fit  $h_0 \propto \sigma^{0.31 \pm 0.02}$ , which is in good agreement with the theory.

## V. Discussion

Figure 8 shows the Langmuir isotherm (a) and the thickness of the brush determined by AFM (b), in a double-logarithmic representation. The  $x$ -axis is the same for both graphs. A single regime is observed on the isotherm when the thickness of the brush varies nonmonotonically. How can we explain this discrepancy between the lateral and normal compression force measurements? To elucidate this, we consider each regime (I), (II), and (III) separately.

In region (I), the surface pressure of the brush is too small to be analyzed, and the thickness of the brush is constant. In section IV, we explained this by the noninteraction of the chains, which is consistent with a very small surface pressure.

In region (II), the surface pressure scales as  $\sigma^{-2}$ , which has been explained as a behavior of quenched polyelectrolyte brush in the strong screening regime. At the same time, the thickness of the brush increases with decreasing the area per chain. Now, by considering eq 10 in section III, we can see that the thickness of a "salted" brush is expected to scale as  $\sigma^{-1/3}$ . Unfortunately, region (II) is not large enough to fit the data with a scaling function. We can only conclude that the increase in the brush thickness is consistent with the behavior of a quenched polyelectrolyte brush in the "salted" regime. With the values of  $h_0$  and  $\sigma$  in the Figure 8b, we can calculate the counterions' concentration in the brush and compare it with the concentration of  $H^+$  ions ( $C_{H^+} = 10^{-2}$  M) to confirm the strong screening regime assumption, i.e.,  $\alpha c_p \ll C_{H^+}$ . The counterions concentration is given by  $\alpha c_p = \alpha N \sigma h_0$ . Replacing  $\alpha$  by the value obtained from the isotherm ( $\alpha = 0.12$ ) gives  $\alpha c_p = 1.4 \times 10^{-2}$  M at  $117.2 \text{ nm}^2$  per

**Table 1.** Calculated Values of the Brush Charge Fraction  $\alpha$  and the Counterions Concentration  $\alpha c_p$  in the Osmotic Regime<sup>a</sup>

area per chain (nm <sup>2</sup> )	$\alpha$	$\alpha c_p$ (10 <sup>-2</sup> M)
19	0.037	4.2
26.9	0.047	3.6
35	0.056	3.2
50	0.071	2.3
80	0.097	1.8
117.25	0.12	1.4

<sup>a</sup> The  $\alpha$  values have been obtained with eq 14 of section III, and the monomer concentrations  $c_p$  have been calculated from the  $h_0$  and  $\sigma$  values read in Figure 8b.

chain,  $\alpha c_p = 1.37 \times 10^{-2}$  M at  $150 \text{ nm}^2$ , and  $\alpha c_p = 1.37 \times 10^{-2}$  M at  $200 \text{ nm}^2$ . These values are of the same order of magnitude as  $C_{H^+}$ . Therefore, even if we are not in the strong screening limit  $\alpha c_p \ll C_{H^+}$ , we can still consider that the salt concentration is high enough to have an effect on the brush behavior.

In region (III), the surface pressure still scales as  $\sigma^{-2}$ , but the thickness of the brush decreases with decreasing the area per chain. We saw in section IV that the variation of  $h_0$  could be fitted with Zhulina's theory for annealed polyelectrolyte brushes in the osmotic regime. Thus, the brush would be a "salted" and quenched brush in region (II) and would become an "osmotic" and annealed brush at high grafting densities. To determine whether the brush is in the osmotic regime in region (III), we can calculate the counterions concentration as above and check that the obtained values are consistent with the conditions  $\alpha c_p \gg (C_S + C_{H^+})$  and  $\alpha \ll 1$ . In this region, the charge fraction is given by eq 14 (cf. section III). The charge fraction should be continuous at the crossover between the two regimes, imposing  $\alpha = 0.12$  at  $117.2 \text{ nm}^2$  per chain. By replacing  $\alpha$  by this latest value in eq 14, we can calculate the charge fraction  $\alpha_B$  of a single PVP chain in the bulk. We obtain  $\alpha_B = 0.14$ . Then, we can calculate the charge fraction and the counterions' concentration for each area per chain of region (III). The corresponding results are shown in Table 1. The values of  $\alpha$  are very small compared to unity, and the counterions concentration values are higher than  $C_{H^+}$ . Nevertheless, one has to note that only the condition  $\alpha c_p > C_{H^+}$  is fulfilled and not the condition  $\alpha c_p \gg C_{H^+}$ . The brush is obviously at the frontier between the "salted" and "osmotic" regimes. It is never in the limit cases  $\alpha c_p \ll C_{H^+}$  or  $\alpha c_p \gg C_{H^+}$  for which the theoretical predictions have been made. This could explain the discrepancy between the AFM measurements and the Langmuir isotherms. For instance, in region (III), where the osmotic regime begins, the surface pressure may not scale as  $\sigma^{-1/3}$  as predicted for the asymptotic case  $\alpha c_p \gg C_{H^+}$ .

## VI. Conclusion

We have investigated annealed polyelectrolyte brushes at pH 2 by combining the Langmuir techniques and the AFM force measurements. The Langmuir isotherm shows that the brush behaves as a quenched one in the "salted" regime. The thickness of the brush obtained from the AFM force-distance curves reveals the existence of three regimes. At low grafting densities, the chains do not interact and the brush thickness is constant. As the grafting density is increased, the thickness of the brush increases, which is consistent with the "salted" regime shown by the isotherm. Finally, at high grafting densities, the thickness of the brush

decreases when the area per chain is decreased. The variations of the thickness in this region is well described by the theoretical predictions of Zhulina et al. for annealed polyelectrolyte brushes in the "osmotic" regime. Nevertheless, we have shown that the brush is neither in the "strong screening" nor in the "osmotic" limit, but rather at the crossover between these two regimes. A better understanding of these systems requires an extension of this study to other pH, ionic strengths, and molecular weights. Moreover, to describe the normal compression force, new theoretical developments are necessary, in which the nonelectrostatic interactions between monomers and the inhomogeneous distribution of the charges along the chain should be taken into account.

**Acknowledgment.** We thank J-F. Joanny (ICS, Strasbourg) for helpful and illuminating discussions on the behavior of polyelectrolyte brushes.

## References and Notes

- (1) Alexander, S. *J. Phys. (Paris)* **1977**, 38, 983.
- (2) de Gennes, P.-G. *Macromolecules* **1980**, 13, 1069.
- (3) Milner, S. T.; Witten, T. A.; Cates, M. E. *Europhys. Lett.* **1989**, 5, 413.
- (4) Milner, S. T.; Witten, T. A.; Cates, M. E. *Macromolecules* **1988**, 21, 2610.
- (5) Birshtein, T. M.; Zhulina, E. B. *Polymer* **1984**, 25, 1453.
- (6) Zhulina, E. B. *Polym. Sci. USSR* **1984**, 26, 885.
- (7) Tirrell, M.; Patel, S.; Hadzioannou, G. *Proc. Natl. Acad. Sci. U.S.A.* **1987**, 84, 4725.
- (8) Hadzioannou, G.; Patel, S.; Granick, S.; Tirrell, M. *J. Am. Chem. Soc.* **1986**, 108, 2869.
- (9) Klein, J.; Luckhman, P. F. *Macromolecules* **1984**, 17, 1041.
- (10) Klein, J.; Luckhman, P. F. *Colloids Surf.* **1984**, 10, 65.
- (11) Pincus, P. *Macromolecules* **1991**, 24, 2912.
- (12) Ross, R. S.; Pincus, P. *Macromolecules* **1992**, 25, 2177.
- (13) Misra, S.; Varanasi, S.; Varanasi, P. P. *Macromolecules* **1989**, 22, 4173.
- (14) Miklavic, S. J.; Marcelja, S. *J. Phys. Chem.* **1988**, 92, 6718.
- (15) Zhulina, E. B.; Borisov, O. V.; Birshtein, T. M. *J. Phys. II* **1992**, 2, 63.
- (16) Borisov, O. V.; Birshtein, T. M.; Zhulina, E. B. *J. Phys. II* **1991**, 5, 63.
- (17) Misra, S.; Varanasi, S. J. *Colloid Interface Sci.* **1991**, 46, 251.
- (18) Lyatskaya, Y. V.; Leermakers, F. A. M.; Fleer, G. J.; Zhulina, E. B.; Birshtein, T. M. *Macromolecules* **1995**, 28, 3562.
- (19) Zhulina, E. B.; Borisov, O. V. *J. Chem. Phys.* **1997**, 107, 5952.
- (20) Israels, R.; Leermakers, F.; Fleer, G. J. *Macromolecules* **1994**, 27, 3087.
- (21) Raphael, E.; Joanny, J.-F. *Europhys. Lett.* **1990**, 13, 623.
- (22) Zhulina, E. B.; Birshtein, T. M.; Borisov, O. V. *Macromolecules* **1995**, 28, 1491.
- (23) Patel, S. S.; Tirrell, M. *Annu. Rev. Phys. Chem.* **1989**, 40, 595.
- (24) Auroy, P.; Mir, Y.; Auvray, L. *Phys. Rev. Lett.* **1992**, 69, 93.
- (25) Mir, Y. Thesis, Université Paris VII, Paris, France, 1995.
- (26) Tran, Y. Thesis, Université Paris VI, Paris, France, 1998.
- (27) Ahrens, H.; Förster, S.; Helm, C. *Phys. Rev. Lett.* **1998**, 19, 4172.
- (28) Zhu, J.; Eisenberg, A.; Lennox, R. B. *J. Am. Chem. Soc.* **1991**, 113, 5585. Zhu, J.; Eisenberg, A.; Lennox, R. B. *Macromolecules* **1992**, 25, 6556.
- (29) Huguenard, C. Thesis, Université Louis Pasteur, Strasbourg, France, 1993.
- (30) Ouahes, R.; Dévallez, B. *Chimie Générale*; Editions PubliSud, 1982.
- (31) Elaissari, A.; Pefferkorn, E. *J. Colloid Interface Sci.* **1990**, 141, 522.
- (32) Manning, G. *J. Chem. Phys.* **1969**, 51, 924.
- (33) Langmuir, I.; Schaefer, V. J. *J. Am. Chem. Soc.* **1938**, 60, 1351.
- (34) Senden, T. J.; Ducker, W. A. *Langmuir* **1994**, 10, 1003.
- (35) Bringuier, E. *J. Phys. (Paris)* **1984**, 45, L-107.
- (36) Witten, T.; Pincus, P. *Europhys. Lett.* **1987**, 3, 315.
- (37) Kumaki, J. *Macromolecules* **1988**, 21, 749.
- (38) Williams, C., private communication.
- (39) Castelnovo, M.; Sens, P.; Joanny, J.-F. *Eur. Phys. J. B*, to be published.

MA991888I